

# Technical Procedures Bulletin

**Subject: Changes to the 2001  
NCEP Operational MRF/AVN  
Global Analysis/Forecast System**

Series No. 484

---

Program and Plans Division,

Silver Spring, MD 20910

---

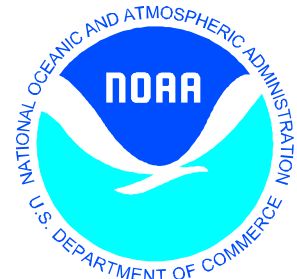
**Abstract:**

The Bulletin was written by Shrinivas Moorthi, Hua-Lu Pan and Peter Caplan of the National Weather Services' National Centers for Environmental Prediction, Global Modeling Branch. It describes the changes to the Medium Range Forecast model on May 15, 2001.

The major changes were in parameterization of cloud material, modification of the radiation heat loss from clouds and modifications to the analysis methodology.



Paul Hirschberg  
Chief, Science Plans Branch



## Changes to the 2001 NCEP Operational MRF/AVN

### Global Analysis/Forecast System:

Shrinivas Moorthi, Hua-Lu Pan and Peter Caplan  
National Centers for Environmental Prediction  
Global Modeling Branch  
W/NP23, World Weather Building,  
Washington DC 20233, USA

#### 1. Introduction.

On 15 May 2001, changes to the following areas in the MRF analysis/forecast system were implemented:

##### Physics

- Inclusion of cloud condensate as a history variable
- Use of the cloud condensate in the calculation of radiative transfer
- Inclusion of cumulus momentum mixing

##### Analysis

- Stronger quality control for AMSU radiances
- Refinement of the hurricane relocation algorithm

This package of changes has produced improvement in circulation patterns in both the extratropics and the tropics, and a significant reduction of the false alarm rate for tropical storms. It has also changed significantly the model's temperature bias.

#### 2. Prognostic cloud condensate.

The computer code for the NCEP operational global spectral model is designed in such a way that a number of tracers can be prognostic quantities. The prognostic tracers used in the present operational model are the specific humidity and ozone mixing ratio, while the experimental model has an additional tracer, namely, the cloud condensate mixing ratio. Cloud condensate is represented as a spectral variable and its three-dimensional advection is treated in the same fashion as any other tracer in the global model.

The equation governing the evolution of cloud condensate can be written as

$$\frac{\partial q_c}{\partial t} = -V \cdot \nabla q_c - \sigma \frac{\partial q_c}{\partial \sigma} + S_c - P - E + F_{qc}$$

where  $q_c$  is the cloud condensate mixing ratio (which can be either liquid water or ice, depending on local temperature),

the first two terms on the right-hand side are the three-dimensional advection,  $S_c$  is the source of  $q_c$  through convective processes,  $S_g$  is the source of  $q_c$  through grid-scale condensation,  $P$  is the rate of conversion of  $q_c$  to precipitation,  $E$  is the evaporation rate of cloud condensate, and  $F_{qc}$  is the horizontal and vertical diffusion.

The convective source term  $S_c$  is provided by the cloud top detrainment in the convective parameterization. The large-scale condensation  $S_g$  is based on Zhao and Carr (1997), which in turn is based on Sundqvist et al.(1989). The precipitation rate  $P$  is parameterized following Zhao and Carr (1997) for ice, and Sundqvist et al.(1989) for liquid water. Evaporation of the cloud condensate also follows Zhao and Carr (1997).

The fractional area of the grid box covered by the cloud is computed diagnostically following the approach of Xu and Randall (1996) using the formula

$$C = \max \left[ R^{0.25} \left( 1 - \exp - \frac{2000x(q_c - q_{cmin})}{\min [\max ([(1-R)q^*]^{0.25}, 0.0001), 1.0]} \right), 0.0 \right]$$

where  $R$  is the relative humidity,  $q^*$  is the saturation specific humidity and  $q_{cmin}$  is a minimum threshold value of  $q_c$ . The saturation specific humidity is calculated with respect to water phase or ice phase depending on the temperature. Unlike the operational model, the new model has only one type of cloud cover represented by  $C$ . In the tropics the cloudiness is primarily due to convective anvils, the result of cumulus detrainment, whereas in the extratropics, cloudiness is mainly through grid-scale condensation.

The fractional cloud cover  $C$  is available at all model levels. There is no cloud cover if there is no cloud condensate. In the operational model's radiation scheme, clouds are assumed to be maximally overlapped if adjacent layers are cloudy. In the prognostic cloud condensate version, clouds in all layers are assumed to be randomly overlapped. Other options will be explored in the future.

The radiation parameterization is also appropriately modified to make use of the predicted cloud condensate in the cloud-radiation interaction. The operational model calculates cloud optical thickness as a function of layer temperature and pressure thickness based on Harshvardhan et al. (1989). The new shortwave radiation follows the approach of Slingo (1989), Chou et al.(1998) and Kiehl et al.(1998) and calculates the optical thickness from the predicted cloud condensate path. The new scheme parameterizes the cloud

single-scattering properties as a function of effective radius of the cloud condensate. The extinction coefficient, the single-scattering albedo and asymmetry factor for a broad band are parameterized as a linear function of the effective radius. The cloud optical thickness then depends on the extinction coefficient and cloud condensate path. The effective radius for ice is taken as a linear function of temperature decreasing from a value of 80 microns at 263.16 K to 20 microns at temperatures at or below 223.16K. For water droplets with temperatures above 273.16 K an effective radius of 5 microns is used, and for supercooled water droplets between the melting point and 253.16 K, a value between 5 and 10 microns is used.

In the present version of solar radiation there are seven UV bands, one visible band and a choice of one or three IR bands. Currently the one IR-band version is being used for computational economy, but in the future the three-band version may be used. Improved versions of parameterizations of aerosol effects and atmospheric absorption due to oxygen are used in an attempt to reduce solar flux reaching the ground. For the infrared radiation, the cloud emissivity is calculated from the predicted cloud condensate following the approach of the NCAR CCM (Kiehl et al. 1998, Stephens (1984).

### 3. Convection

The MRF has suffered from a false-alarm problem in its tropical storm forecasts during the past few years, too often making initially weak tropical disturbances into stronger storms 3-5 days into the forecast. The mechanism responsible for limiting the growth of the storms is believed to be the interaction between the convection and the vertical wind shear in the environment. While the Simplified Arakawa-Schubert scheme in the operational MRF model includes wind shear considerations in the downdraft computation, the momentum field is not altered by convection.

In the upgrade to be implemented, mass fluxes induced in the updraft and the downdraft are allowed to transport momentum. The momentum exchange is calculated through the mass flux formulation in a manner similar to that for heat and moisture. In order to take into account the pressure gradient effect on momentum, a simple parameterization using entrainment is included for the updraft momentum inside the cloud.

The entrainment rate, tuned to ensure that the tropical easterly jet strength in the Indian monsoon flow maintains the least drift in the forecast is set to 1/km. This addition to the cumulus parameterization has reduced the feedback between heating and circulation in sheared flows.

In addition, we have made a change in the cloud top selection algorithm in the convection parameterization. In the current SAS scheme, the cloud top level is determined by the parcel method. The level where the parcel becomes stable with respect to the environment is the cloud top. When the prognostic

cloud water scheme is tested with this scheme, there is evidence that cloud top detrainment is too concentrated in the upper troposphere. In order to provide a more even detrainment of cloud water in the tropics, we have made a change to the selection algorithm. Once the highest possible cloud top has been determined by the parcel method, we make a random selection of the actual cloud top between the highest possible cloud top and the level where environmental moist static energy is a minimum. The proper entrainment rate is computed to ensure that the parcel becomes neutral at the new cloud top. This is very similar to the Relaxed Arakawa-Schubert (RAS) scheme developed by S. Moorthi.

#### 4. Analysis changes.

Two minor analysis changes are included in this package.

a. An additional quality control test for AMSU-A radiances has been added to screen out observations whose simulated brightness temperatures are highly sensitive to the surface emissivity. The effect of this test is largely limited to observations over water surfaces in the presence of high low-level wind speeds.

b. The tropical storm relocation algorithm has been refined as follows:

- (1) the land/sea mask is not checked;
- (2) over mountains >500m in elevation only the wind field is relocated;
- (3) hurricane positions at -3h and +3h are estimated based on the difference between the model position and the observed position at 0h.

#### 5. Impact of the changes on model behavior.

The major components of the package to be implemented were tested separately and then together in daily runs parallel to the operational system in more or less final form, from about October, 2000 through May, 2001, during most of which period the forecasts were available for daily inspection by the staff in HPC as supplemental input into national guidance and to personnel in other branches who attend the daily map discussions. In addition, retrospective runs for May through mid-June of 1999 were made and evaluated by HPC personnel, including the South American Desk. Finally, retrospective runs covering part of the 2000 hurricane season were made available to the Tropical Prediction Center.

The general consensus of the subjective evaluations coming out of these runs was that the most noticeable features of the new model include

- a. Reduction of the frequency and strength of tropical storms, eliminating many false alarms

- b. Replacement of the warm bias near the surface with a cold bias
- c. Decreased intensity of cut-off circulations in the extratropics and a related loss of transient-eddy kinetic energy in the upper troposphere

## 6. Model performance statistics vs. analysis

In evaluations of predicted wind and mass fields against verifying analyses, the new package showed consistent improvement over the operational for both the summer/autumn and the winter tests. The 500-hPa anomaly correlation dieoff curves for the first period, October 6-December 14, 2000 are shown in Fig. 1a for the Northern Hemisphere and Fig. 1b for the Southern Hemisphere. The corresponding curves for the period 15 Dec 2000 through 27 Feb 2001, given in Fig. 2a and Fig. 2b show the same general picture. The new model (MRFY, green) gets better scores on average at all forecast lengths out to 9 days, in both hemispheres, for all wave number groups shown, and in both seasons tested. In addition, the improvement of the new package over the operational makes up a significant portion of the gap between the operational and the ECMWF (red) in the extratropics.

Verifications of three-day forecasts of winds at two levels in the tropics, shown in Fig. 3, reveal a consistent reduction in

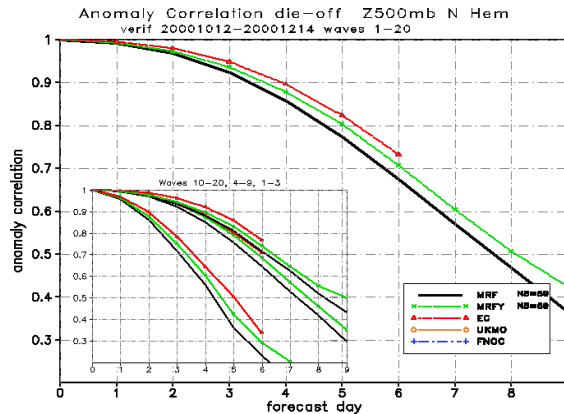


Fig.1a. AC vs time, 3 models, 3 wave no. groups, N. Hemisphere.

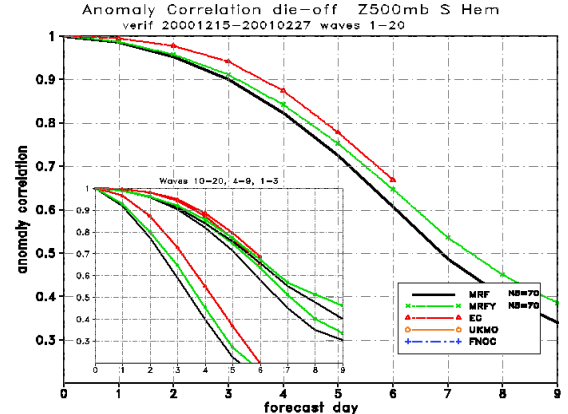


Fig. 1b. As in 1a, but for S..Hemisphere.

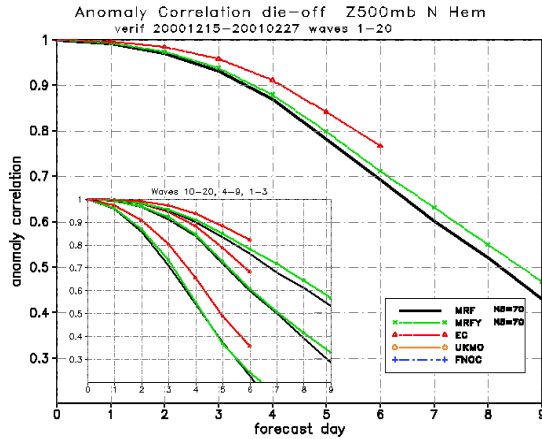


Fig. 2a. As in 1a, but for Dec-Feb.

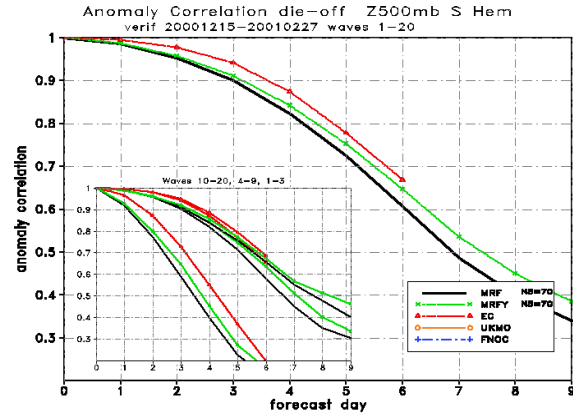


Fig. 2b. As in 2a, but for S. Hemisphere.

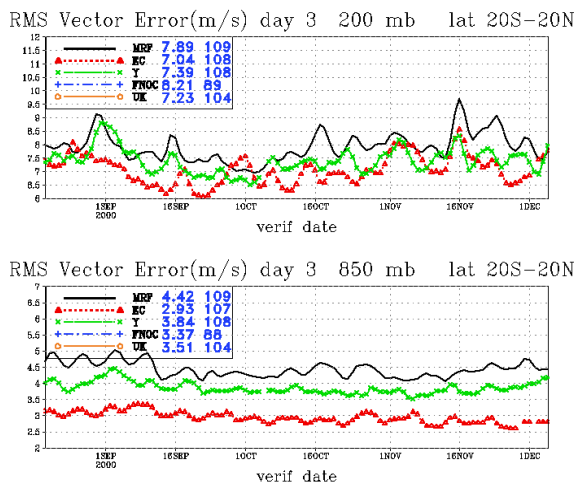


Fig. 3. RMS vector wind error, day 3, 200 and 850 hPa, tropics. New model in green, averages in inset

vector wind errors against rawinsonde observations in the extratropics averaged over April, 2001 for forecasts to 2 days are plotted in Fig. 4a for the operational model and Fig. 4b for the new model. The errors are only slightly smaller in the new model, probably because only the first two forecast days were considered.

In spite of its good scores for mass and wind forecasts, the new model has problems with temperature bias. The vertical distributions of the temperature errors verified against rawinsondes averaged over the Northern Hemisphere for March, 2001 are shown in Fig. 4c for the old model and Fig. 4d for the new model.

It is clear that even though the rms error has not been much affected, there has been an increase and change in sign of the bias, apparent even early in the forecast. This is consistent with the distribution of the day 5 temperature errors with

error, averaging about 0.6 m/sec at both levels. Although a significant part of the error reduction at 850 hPa does come from a negative speed bias at that level, the reduction of the error reflects the important reduction in spurious tropical circulations brought about by the implementation of cumulus momentum mixing.

## 7. Verifications against rawinsondes

Vertical distributions of rms

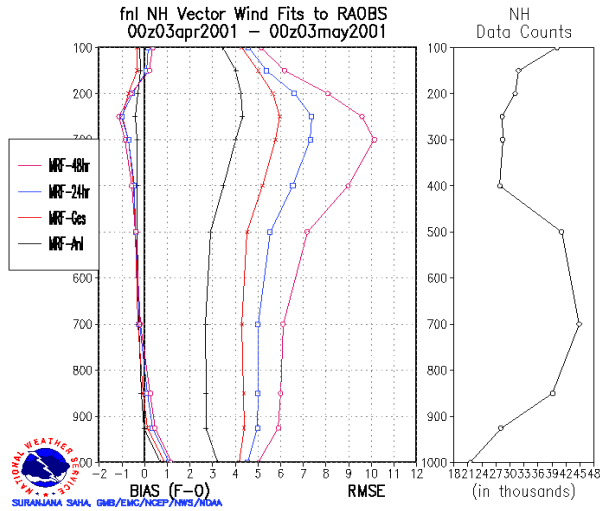


Fig.4a. Wind error vs obs, NH, bias (l), rms vector error (r), anl, ges, day 1, day 2, April, 2001, old model.

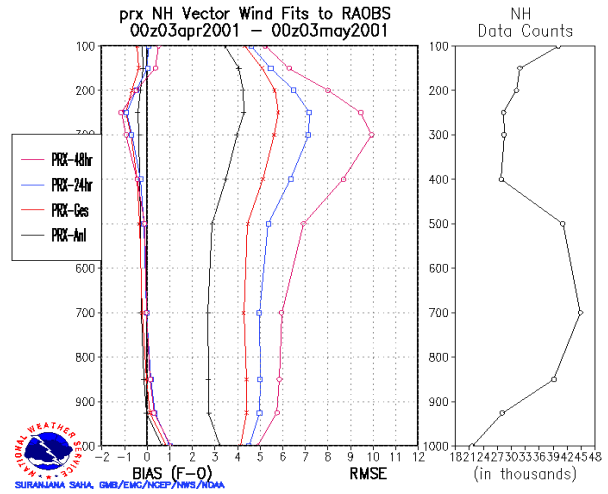


Fig. 4b. As in 4a, but for new model.

latitude

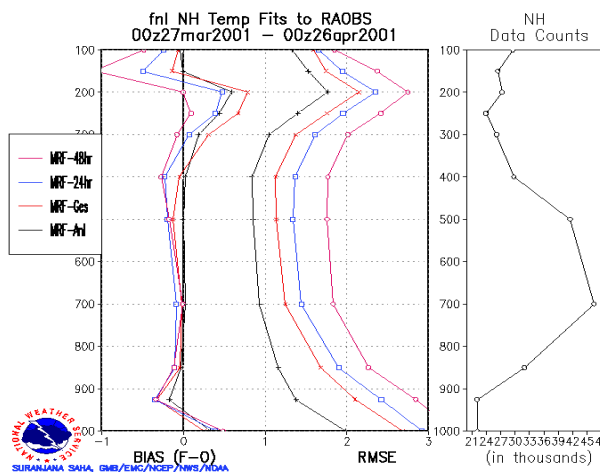


Fig.4c. As in 4a, but for temperature bias and rms error, old model.

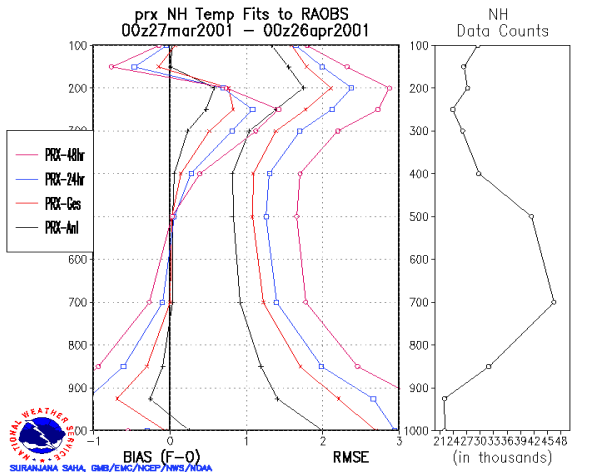


Fig. 4d. As in 4c, but for new model.

latitude in the error pattern against analyses, shown in the vertical cross section in Fig. 4e. In this diagram old is above, new below. The distribution over the U.S. of 850-hPa temperature errors vs observations for the analysis, guess, and 12-h, 24-h, 36-h and 48-h forecasts during April, 2001 is shown in Fig. 4f for the old model and Fig. 4g for the new model. Since the 12-h and 36-h forecasts verify at 12z and the others at 00z, the diurnal dependence of the bias is discernible. Both are somewhat warmer at 00z. During this period, the old model shows a strong diurnal variation of bias, warm during the day, cold at night, while the new model (prx) is always cool in most areas, with the largest biases in the northwest quadrant of the country.



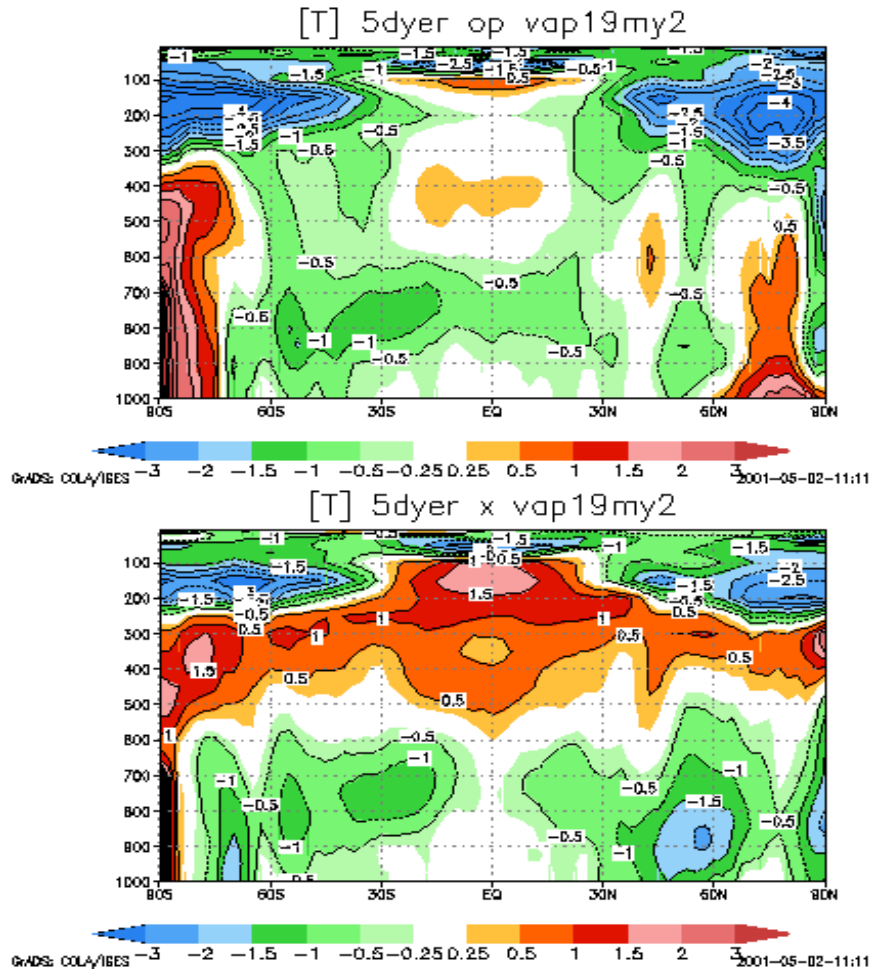


Fig. 4e. Day 5 temperature error, fcst-anl, old modell (top), new (bottom), zonal avg vertical cross-section, 19 Apr-2May avge.

## 8. Precipitation verifications

Based on observations over the Continental U.S., the new model yielded much the same threat scores as the old, but was consistently a bit wetter, usually only for amounts under half an inch.

As an example, threat scores for January, 2001 are shown in Fig. 5a and bias scores in Fig. 5b. The blue curves (MRFY) represent the new model (without the analysis changes), the red lines the old (The green lines are for a test of the analysis changes only).

## 9. Hurricane case

An example of the suppression of a spurious hurricane occurred during tests of the new physics in the Autumn, 2000 hurricane season.

**Temp 850 mb BIAS in Celsius  
from 00z01apr2001-00z30apr2001**

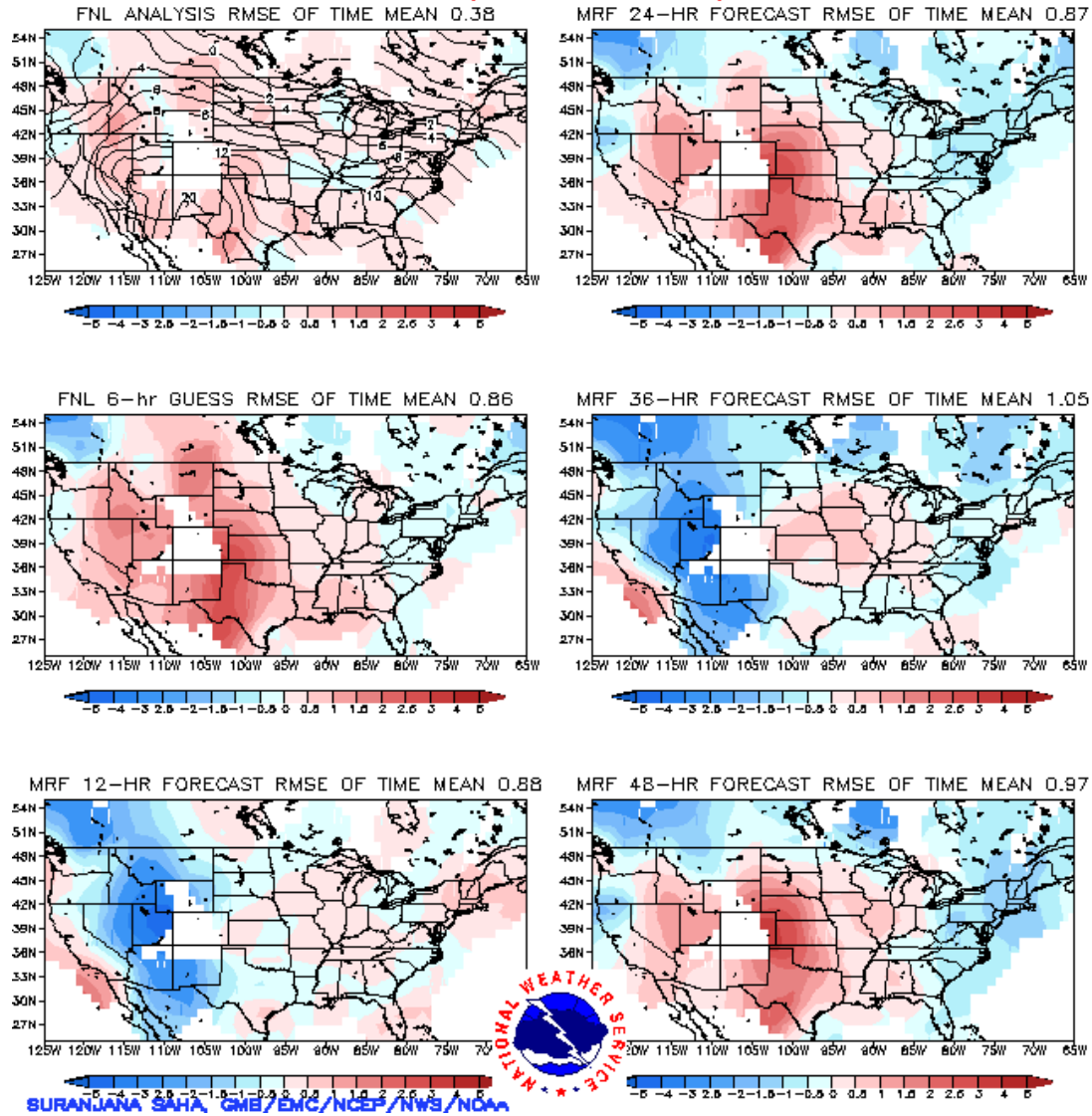


Fig. 4f. 850-hPa temperature bias, old model - rawinsondes, avge for analysis, and 6-h guess and 12-h, 24-h, 36-h and 48-h forecasts verifying April, 2001. Rmse of time mean printed above each panel.

**Temp 850 mb BIAS in Celsius  
from 00z01apr2001-00z30apr2001**

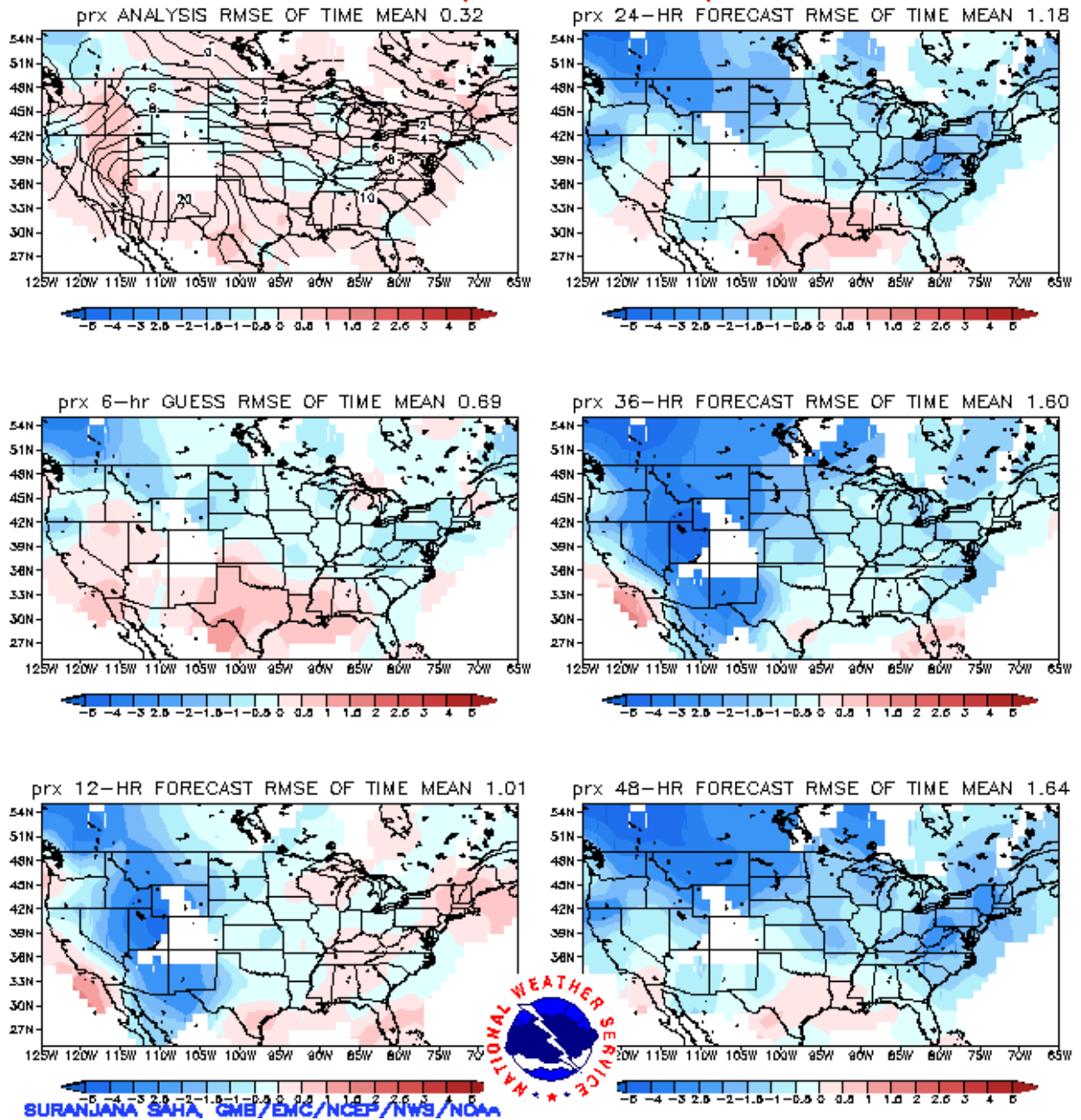


Fig. 4g. As in 4f, but for new model.

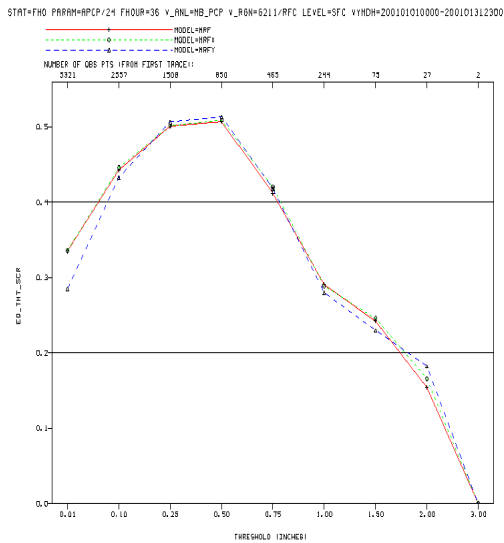


Fig. 5a. Equitable threat scores, Jan 2001 avg for 12-36h as a function of precip amount for old model(black) new model(green) and test model with only analysis changes(blue).

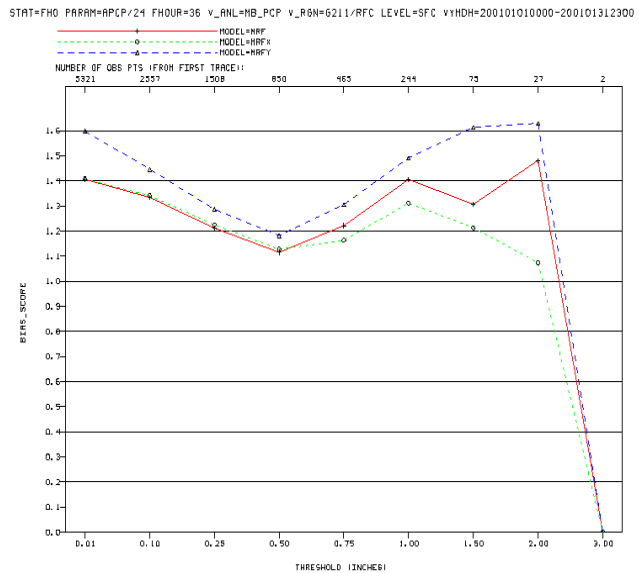


Fig. 5b. As in 5a, but for bias

The 132-h forecast from the old model is shown in Fig. 6a, the new model in Fig. 6b and the verifying analysis in Fig. 6c. In this case a spurious storm in the Eastern Pacific was suppressed, while the real storm in the Atlantic (Alberto) was retained, with a modest loss of intensity.

## 10. Summary and future work

Based on the large number of experimental runs and diagnostic tests conducted our conclusion is that the major changes described above have, on average, significantly improved the accuracy of forecasts of the mass and wind fields. Evaluations from outside of the Environmental Modeling Center of both parallel and retrospective experiments were positive - the new model was found to provide better guidance than the old. A particularly valuable result was the strong reduction in the number of spurious low-level circulations produced in the subtropics and tropics. On the negative side, precipitation forecasts did not show improvement and neither did temperature biases. Also, the model seemed to be losing kinetic energy in its transient eddies over the first week to ten days of the forecast.

It is felt that this implementation will put the model on a firmer and more realistic physical footing, but, as with any major implementation of this sort, tuning and adjusting will be

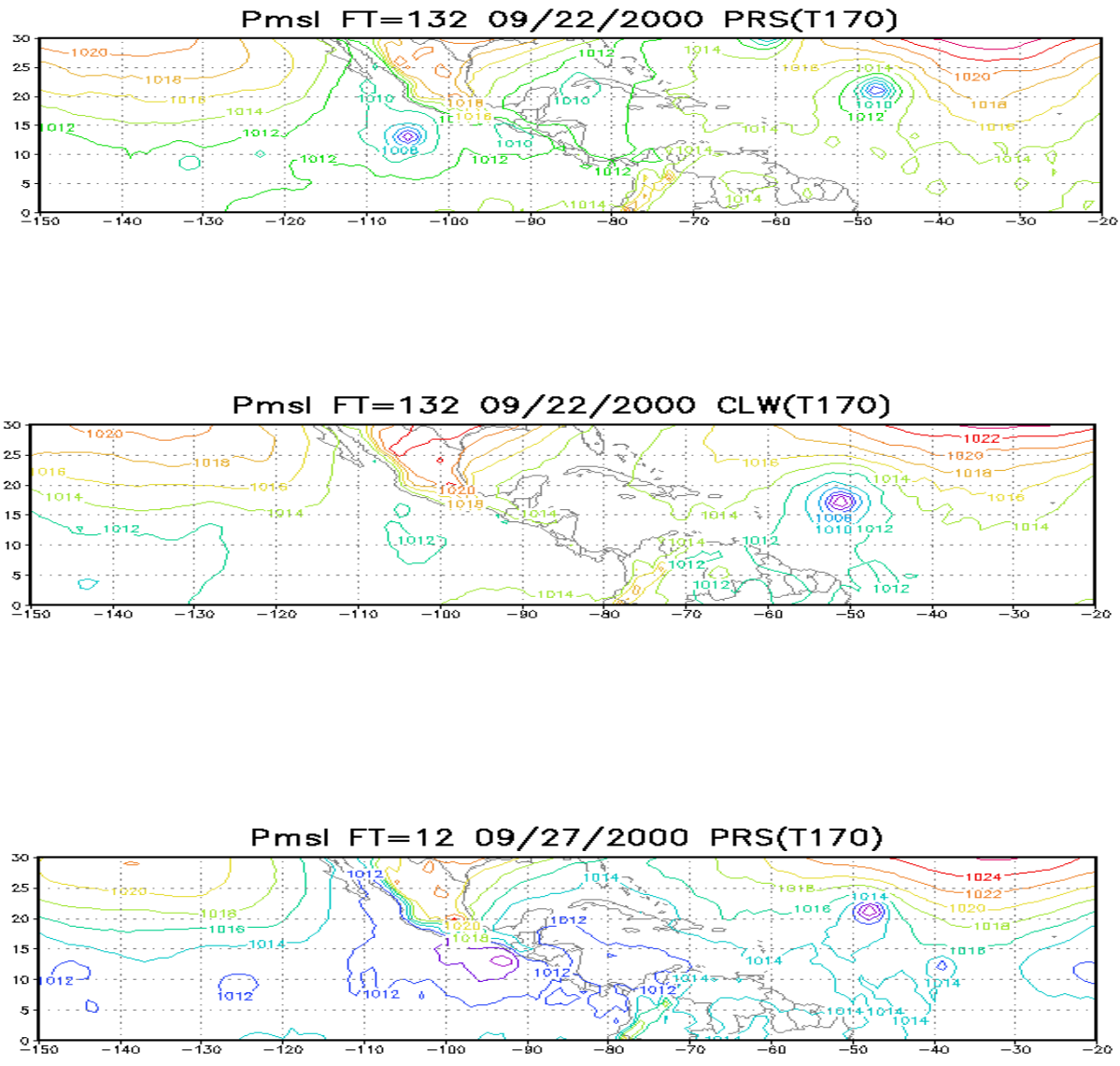


Fig. 6. Top: Isobars of sea level pressure for 132-h forecast from 9/22/2000, old model  
 Middle: Same for new model.  
 Bottom: As above, but for verifying analysis, 9/27/2000

necessary before the full value of the changes is realized. Of necessity, this process could not be carried out during the

lengthy period during which the system had to be frozen for pre-implementation testing and evaluation by the field, but it will begin as soon as possible.

#### References.

Chou, M.D., M. J. Suarez, C. H. Ho, M. M. H. Yan, and K. T. Lee, 1998: Parameterizations for cloud overlapping and shortwave single scattering properties for use in general circulation and cloud ensemble models. *J. Climate*, 11, 202-214.

Harshvardhan, D. A. Randall, T. G. Corsetti, and D. A. Dazlich, 1989. Earth radiation budget and cloudiness simulations with a global general circulation model. *J. Atmos. Sci.*, 46, 1922-1942.

Kiehl, J.T., J. J. Hack, G. B. Bonan, B. A. Boville, D. L. Williamson, and P. J. Rasch, 1998: The national center for atmospheric research community climate model CCM3. *J. Climate*, 11, 1131-1149.

Slingo, A., 1989: A GCM parameterization for the shortwave radiative properties of water clouds. *J. Atmos. Sci.*, 46, 1419-1427.

Stephens, G. L., 1984: The parameterization of radiation for numerical weather prediction and climate models. *Mon. Wea. Rev.*, 112, 826-867.

Sundqvist, H., E. Berge, and J. E. Kristjansson, 1989: Condensation and cloud studies with mesoscale numerical weather prediction model. *Mon. Wea. Rev.*, 117, 1641-1757.

Xu, K. M., and D. A. Randall, 1996: A semiempirical cloudiness parameterization for use in climate models. *J. Atmos. Sci.*, 53, 3084-3102.

Zhao, Q. Y., and F. H. Carr, 1997: A prognostic cloud scheme for operational NWP models. *Mon. Wea. Rev.*, 125, 1931-1953.